Eur Radiol (2009) 19: 1223–1231
DOI 10.1007/s00330-008-1253-x

Mario Alerci
Michel Oberson
Antonella Fogliata
Augusto Gallino
Peter Vock
Rolf Wyttenbach

Prospective, intraindividual comparison of MRI versus MDCT for endoleak detection after endovascular repair of abdominal aortic aneurysms

Received: 3 July 2008
Revised: 28 September 2008
Accepted: 29 October 2008
Published online: 23 December 2008

M. Alerci · R. Wyttenbach (✉)
Department of Radiology, Ospedale San Giovanni Bellinzona (EOC), 6500 Bellinzona, Switzerland
e-mail: rolf.wyttenbach@bluewin.ch
Tel.: +41-91-8118662
Fax: +41-91-8118656

M. Oberson · A. Gallino
Department of Cardiology, Ospedale San Giovanni Bellinzona (EOC), Bellinzona, Switzerland

A. Fogliata
Department of Medical Physics, Ospedale San Giovanni Bellinzona (EOC), Bellinzona, Switzerland

P. Vock
Department of Radiology, Inselspital, University of Berne, Berne, Switzerland

Abstract This study compares MRI and MDCT for endoleak detection after endovascular repair of abdominal aortic aneurysms (EVAR). Forty-three patients with previous EVAR underwent both MRI (2D T1-FFE unenhanced and contrast-enhanced; 3D triphasic contrast-enhanced) and 16-slice MDCT (unenhanced and biphasic contrast-enhanced) within 1 week of each other for endoleak detection. MRI was performed by using a high-relaxivity contrast medium (gadobenate dimeglumine, MultiHance®). Two blinded, independent observers evaluated MRI and MDCT separately. Consensus reading of MRI and MDCT studies was defined as reference standard. Sensitivity, specificity, and accuracy were calculated and Cohen's *k* statistics were used to estimate agreement between readers. Twenty endoleaks were detected in 18 patients at consensus reading (12 type II and 8 indeterminate endoleaks). Sensitivity, specificity, and accuracy for endoleak detection were 100%, 92%, and 96%, respectively, for reader 1 (95%, 81%, 87% for reader 2) for MRI and 55%, 100%, and 80% for reader 1 (60%, 100%, 82% for reader 2) for MDCT. Interobserver agreement was excellent for MDCT (k=0.96) and good for MRI (k=0.81). MRI with the use of a high-relaxivity contrast agent is significantly superior in the detection of endoleaks after EVAR compared with MDCT. MRI may therefore become the preferred technique for patient follow-up after EVAR.

Keywords Aneurysm · Aorta · Endovascular repair · Endoleak · Computed tomography · Magnetic resonance imaging · Gadobenate dimeglumine

Abbreviations MDCT: multidetector computed tomography · MRI: magnetic resonance imaging · EL: endoleak(s) · EVAR: endovascular aortic aneurysm repair · MRA: magnetic resonance angiography · MPR: multiplanar reconstruction · MIP: maximum-intensity projection · CI: confidence interval

Introduction

Endovascular repair of aortic aneurysms (EVAR) was introduced by Parodi et al. [1] and has subsequently emerged as a viable alternative to open surgery for selected patients with abdominal aortic aneurysms [2]. At present life-long imaging follow-up is essential to evaluate treatment success and to exclude complications related to EVAR such as aneurysm expansion and formation of endoleaks (EL) [3], representing blood flow outside the stent graft lumen but within the aneurysm sac.

Currently, triphasic contrast-enhanced computed tomography (CT) is widely considered to be the most appropriate method for imaging surveillance of patients after EVAR [4] and its validity has been demonstrated by several studies [5–8]. However, sometimes the sensitivity of CT appears to

be insufficient to identify small endoleaks [9]. Accurate identification of endoleaks is crucial since any type of EL may increase pressure within the aneurysm sac and therefore contribute to aneurysm growth or even put the patient at risk of aneurysm rupture [10].

To date, magnetic resonance imaging (MRI) is less frequently used for imaging follow-up in patients after EVAR as an alternative to computed tomography since it is considered time consuming, costly, and not universally available [4]. A few studies suggested that MRI may be more sensitive than CT for the detection of EL [10–12]. However, these studies used single-detector and 4-row multidetector CT (MDCT) and standard gadolinum chelates for MR imaging for endoleak detection.

Gadolinium-BOPTA (gadobenate dimeglumine, MultiHance®, Bracco, Italy) is characterized by a weak protein interaction, leading to an almost twofold increase in relaxivity compared with conventional Gd chelates without protein interaction [13]. This property might potentially be useful for the detection of (low-flow) endoleaks after EVAR, where inadequate opacification with contrast medium represents a major limitation. To our knowledge no previous studies have been published in which Gd-BOPTA is used for the assessment of endoleaks after EVAR.

The purpose of the current study was therefore to perform a prospective, intraindividual comparison between contrast-enhanced MR imaging and 16-slice MDCT for the detection of endoleaks in patients after EVAR by using a high-relaxivity MR contrast medium.

Materials and methods

Patients and study protocol

This prospective study included 43 out of 93 patients that had been treated with endovascular repair of abdominal aortic aneurysms between 1999 and 2007 at our institution. Fifty patients were excluded because of the following reasons: stent grafts not made of nitinol (n=7); follow-up elsewhere (n=4); disagreement to undergo both CT and MRI studies (n=9); claustrophobia (n=5); death (n=4); pacemaker (n=9); renal insufficiency (n=11); allergy to contrast agent (n=1) (Fig. 1).

Each patient gave written informed consent and the study was approved by the local ethics committee. The clinical patient characteristics are provided in Table 1. The mean time after intervention was 35 months ± 23 SD (range 2–88 months). Two different types of nitinol stent grafts were used: Talent (n=13; Medtronic, Sunnyvale, CA) and Excluder (n=30; WL, Gore & Associates, Inc. Flagstaff, AZ). All patients had undergone, if technically possible, embolization of lumbar and/or inferior mesenteric arteries prior to EVAR to reduce the risk of endoleaks, according to the standard protocol used at our institution [14].

All patients, independent of their participation in this study, were part of an imaging surveillance program after EVAR that included abdominal radiographs (anteroposterior, RAO, LAO), Doppler ultrasound, and triphasic contrast-enhanced CT after 2 days, at 3, 6, and 12 months after the intervention and yearly thereafter.

Our study patients (n=43) were therefore part of a follow-up program and underwent, besides the radiographs and computed tomography, an additional contrast-enhanced MRI examination within 1 week of the CT study. No digital subtraction angiography (DSA) was performed. The study was carried out between November 2006 and May 2007.

Multidetector computed tomography

All CT angiography studies were performed on a 16-slice multidetector CT system (Brilliance 16, Philips Medical Systems, Best, Netherlands). Images were obtained using

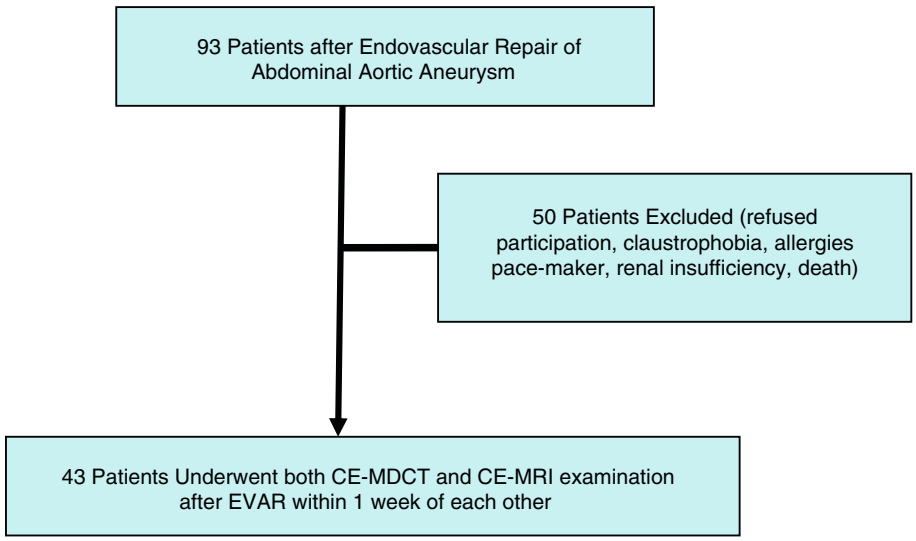

Fig. 1 Outline of the study

Table 1 Clinical characteristics of patients

Characteristic	Value
Total number of patients	43
Males/females	41/2
Age (years)	72.3±8
History of smoking	8
Arterial hypertension	36
Dyslipidemia	30
CAD (angina pectoris and/or prior myocardial infarction)	14
Diabetes	7
Body mass index	27±4
Renal function (eGFR ml/min/1.73 m^2, mean)	74
Range	61–120
Mean aneurysm size (mm)	55×58
Range	50–74
Type of stent graft	
Talent	13
Excluder	30
Mean time after EVAR (months)	35±23

CAD coronary artery disease, *eGFR* estimated glomerular filtration rate
Deviations are reported as ± 1 standard deviation

120 kV, variable mAs (dose modulation), 16×1.5 mm collimation, reconstruction thickness 2 mm, and reconstruction interval 1 mm. CT angiography included one unenhanced CT acquisition followed by acquisitions enhanced by intravenous iodinated contrast material: 120 ml at a flow rate of 4 ml/s, Ioversol 350 mg I/ml (Optiray® 350, Guerbet, Aulnay-sous-Bois, France) administered intravenously by an automated power injector (OptiVantage DH, Mallinckrodt, Zürich, CH) followed by a saline chaser of 30 ml at the same flow rate. Automated timing of the arterial phase acquisition was used (Bolus Tracking, Philips Medical Systems, Best, The Netherlands) by positioning of the region of interest in the abdominal aorta at the level of the celiac trunk. The delayed phase was acquired 60 s after the arterial phase. Coronal and sagittal multiplanar reconstructions (MPR) with a slice thickness of 3 mm were performed interactively on a separate work station (Extended Brilliance Workspace, release 3.5, Philips Medical Systems, Best, Netherlands). In addition, the total patient in-room time, including patient setup and the total described CTA protocol was measured.

Magnetic resonance imaging

All MRI examinations were performed on a 1.5-T whole body MR system (Intera; R 11, Philips Medical Systems, Best, Netherlands) with a gradient strength of 30 mT/m and a slew rate of 150 mT/m/ms. A 4-element phased-array body coil was used for signal reception.

The MRI protocol started with an axial T1-weighted echogradient sequence (FFE, fast field echo) using the following imaging parameters: TR ms/TE ms, 180/1.37; flip angle, 80°; acquired resolution, 1.3×1.8×6.5 mm^3 (reconstructed voxel size, 0.78×0.78×6.5 mm^3); parallel imaging with acceleration (SENSE) factor, 1.8; acquisition time, 18 s.

For contrast-enhanced MR angiography (MRA) the delay before MR acquisition was determined by a test bolus (2 ml and a flow rate of 2.5 ml/s) administered intravenously using a MR-compatible injector (Injektron 82 MRT; Medtron, Saarbrücken, Germany) and a 30 ml saline flush at 2.5 ml/s. Subsequently, a coronal 3D gradient-recalled-echo sequence was performed after the intravenous administration of Gd-BOPTA (gadobenate dimeglumine, MultiHance®, Bracco, Italy) at a dose of 0.15 mmol/kg body weight and a flow rate of 2.5 ml/s followed by a saline flush of 30 ml at the same injection rate. The MRA sequence was performed before contrast medium administration, during the arterial phase and during the late phase starting approximately 30 s after the beginning of the arterial phase.

The following imaging parameters were used for coronal contrast-enhanced MRA: TR ms/TE ms, 3.6/1.2; flip angle, 35°; field of view, 450 mm, rectangular field of view, 90%; matrix, 400×292; number of sections 70; acquired spatial resolution, 1.1×1.5×3 mm^3 (reconstructed voxel size 0.9×0.9×1.5 mm^3); bandwidth, 434 Hz; acquisition time, 17.3 s. Randomly segmented central k-space ordering (i.e., contrast-enhanced timing-robust angiography [CENTRA]) was used [15]. The field of view of 450 mm was chosen to avoid fold over artifacts since parallel imaging was employed with a SENSE factor of 2.

Immediately after the MRA study the unenhanced T1-weighted echogradient sequence was repeated using identical positioning and imaging parameters. Finally, an enhanced T1-weighted echogradient sequence with selective water excitation (Proset) was acquired in order to suppress the signal of fat by using the following imaging parameters: TR ms/TE ms, 321/3.9; flip angle, 80°; Proset pulse type, 121; acquired resolution, 1.3×1.9×6.5 mm^3 (reconstructed voxel size, 0.78×0.78×6.5 mm^3); SENSE factor, 2; acquisition time, 29.5 s (2 breath-holds). All MRI sequences were acquired using the breath-hold technique. In addition, the total patient in-room time, including patient setup with positioning of the phased-array body coil and the total described MRI protocol, was measured.

Postprocessing, reference standard, image analysis

All CT and MRI data were transferred to a PACS system (Easy Access, release 10.2, Philips Medical Systems, Best,

NL) for evaluation. CT and MRI studies were analyzed separately and independently by two experienced, board-certified radiologists with 12 years (R.W.; reader 1) and more than 20 years (M.A.; reader 2) of experience in cross-sectional imaging. Reader 1 (reader 2) first evaluated all MRI (CT) studies in random order and 10 weeks later all CT (MRI) examinations. Both readers were blinded to patient data and to previous cross-sectional studies. All data sets were also available on a workstation (View forum; release 4.1; for MRI studies and Extended Brilliance Workspace, release 3.5, for CT studies; both Philips Medical Systems, Best, NL) permitting review of source images and interactive reformation at the time of analysis, if necessary.

All studies were assessed for the presence of endoleaks, defined as contrast enhancement outside the stent graft lumen, but inside the aneurysm sac. In addition, for MRI studies only a relative extraluminal enhancement of more than 100% compared with precontrast images was considered an endoleak, because smaller signal increase could represent tissue organization rather than endoleak blood flow [16]. All endoleaks were classified as type I–V or as indeterminate endoleaks, if the exact type of endoleak could not be defined (Table 2).

Analysis of the imaging data included measurement of maximum diameters (millimeters) of the aneurysm sac oriented perpendicularly to the centerline of the aorta as assessed on the MPR data sets. Additional measurement of aneurysm size on previous CT studies, obtained according to the surveillance program, was performed to evaluate eventual progression of aneurysm dimensions. Both observers recorded the phases on CT (arterial, late) and the sequences on MRI (MRA arterial, late, T1 FFE, T1 WATS) where the endoleaks were best visualized.

Overall image quality of CT and MRI studies in terms of contrast enhancement, low signal to noise ratio, and artifacts not caused by stent grafts or coils was assessed by a four-point scale as follows: 0, excellent (evaluation possible with high diagnostic confidence); 1, good (evaluation possible with good diagnostic confidence); 2, moderate (evaluation possible with low diagnostic confidence); 3, nondiagnostic (not adequate for analysis).

The grade of artifacts caused by the stent graft or coils in lumbar or inferior mesenteric arteries was categorized as follows on a four-point scale: 0, no artifacts (evaluation possible with high diagnostic confidence); 1, slight artifacts (evaluation possible with good diagnostic confidence); 2, moderate artifacts evaluation possible with low diagnostic confidence); 3, strong artifacts, (not adequate for analysis).

After the independent analysis of the CT and MRI studies, the final diagnostic reference standard was achieved by consensus reading of both imaging techniques in each individual case, utilizing also clinical data and, if available, previous or follow-up studies.

Stent-graft-related complications such as dislocation of the endoprothesis, kinking, or occlusion of the graft were also assessed.

Table 2 Classification of endoleaks

Endoleak type	Source of endoleak
I	Attachment site leak—proximal (Ia) or distal (Ib)
II	Aortic side branches[a]
III	Graft failure—midgraft hole, junctional leak, disconnect
IV	Graft wall porosity
V	Endotension[b]
Indeterminate	Not classifiable as type I–V endoleak

[a]Most commonly lumbar, mesenteric, or iliac collateral vessel leak
[b]Expansion of the aneurysm dimensions without visible endoleak

Statistical analysis

Sensitivity, specificity, accuracy, and negative predictive value (NPV) of MRI and MDCT for detection of EL were calculated using consensus readings of MRI and MDCT studies as the reference standard.

Interobserver agreement for detection of the presence or absence of an endoleak was determined by means of the Cohen's k test, where $k>0.75$ corresponds to an excellent agreement and k between 0.5 and 0.75 corresponds to a good agreement.

For assessment of image quality and artifacts, mean values were calculated and data of MRI and MDCT were compared. For continuous variables, the paired, two-tailed Student's t test was applied; whereas for categorical variables the paired Wilcoxon signed ranks test was used. Differences were considered statistically significant with a p value of less than 0.05. Statistical analysis was performed with SPSS, version 11.5 (SPSS Inc., Chicago IL, USA).

Results

Consensus reading

All 43 MRI and MDCT studies were considered of diagnostic quality. At consensus reading a total of 20 endoleaks in 18 different patients were diagnosed. Out of these 20 EL, 12 were considered type II endoleaks and the remaining 8 EL were classified as indeterminate (Table 3). Six of these indeterminate EL were localized in the central part of the aneurysm sac and 2 EL were found near the proximal anchoring points of the stent grafts.

Table 3 Detection and classification of endoleaks by MRI versus MDCT compared with reference standard

Type of endoleak	MRI reader 1	MRI reader 2	CT reader 1	CT reader 2	Consensus reading
Ia	0	0	0	1	0
Ib	0	0	0	0	0
II	19	13	10	7	12
III	0	0	0	0	0
IV	0	0	0	0	0
V	0	0	1	0	0
Indeterminate	3	11	0	4	8
Total EL	22	24	11	12	20
Patients	19/43	21/43	11/43	12/43	18/43

Consensus reading of CT and MRI studies by both readers was used as reference standard

Endoleak detection by MRI and MDCT

Detailed data on the detection of EL by both readers on MRI and MDCT studies are provided in Table 3 and Figs. 2, 3, 4.

Compared with consensus reading MRI showed a sensitivity, specificity, accuracy, and negative predictive value (NPV) for endoleak detection of 100% [95% confidence interval (CI) 90–100%], 92% [95% CI 84–100%], 96% [95% CI 90–100%] and 100% [95% CI 92–100%] for reader 1 and 95% [95% CI 85–100%], 81% [95% CI 74–88%], 87% [95% CI 81–93%], and 96% [95% CI 87–100%], respectively, for reader 2. More details are provided in Table 4.

Sensitivity, specificity, accuracy, and NPV for endoleak detection on multidetector computed tomography were 55% [95% CI 47–63%], 100% [95% CI 92–100%], 80% [95% CI 75–85%], and 74% [95% CI 68–79%] for reader 1 and 60% [95% CI 52–68%], 100% [95% CI 92–100%], 82% [95% CI 77–88%], and 76% [95% CI 70–81%] for reader 2. In total, reader 1 diagnosed 20 of 20 EL [100%] on MRI and 11 of 20 EL [55%] on CT. Reader 2 detected 19 of 20 EL [95%] on MRI and 12 of 20 [60%] on CT. Differences between the number of detected endoleaks by MRI versus CT were significant for both observers ($p<0.01$). Computed tomography produced a considerable number of false negative findings with 9 of 20 EL missed by reader 1 (8 by reader 2). On MRI, 2 false positive findings were reported by reader 1 (5 by reader 2), and only 1 false negative by reader 2. There were a relatively high number of endoleaks that could not be classified into categories I–V and these were therefore considered as indeterminate (Table 3). Two indeterminate EL missed on CT were only seen on late postcontrast (T1 echogradient and T1 echogradient Proset) MRI images.

The interobserver agreement for the detection of endoleaks was excellent for MDCT ($k=0.96$) and good to excellent for MRI ($k=0.81$).

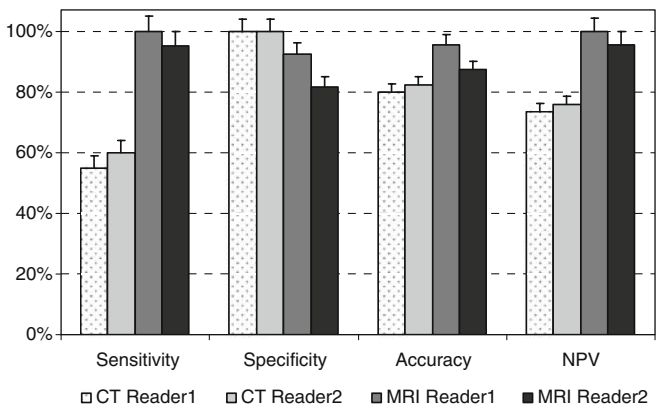

Fig. 2 Graph demonstrates sensitivity, specificity, accuracy, and negative predictive value (NPV) of multidetector CT versus MRI for readers 1 and 2 in the detection of endoleaks after EVAR. *Error bars* are values of standard deviation. Note the significantly higher sensitivity and NPV of MRI compared with CT for the detection of endoleaks for both readers

Acquisition technique and aneurysm dimensions

With respect to the acquisition technique, endoleaks were best visualized on CT in the late contrast-enhanced phase for both readers (11/11 EL [100%] for reader 1 and 12/12 [100%] for reader 2), whereas 2/11 [18%] and 3/12 [25%] endoleaks were not detected on the arterial phase CT studies by observer 1 and 2, respectively.

On MRI, reader 1 detected 17/23 [74%] endoleaks (reader 2, 17/24 [71%]) on late contrast-enhanced T1 (FFE and WATS), 12/23 [52%] EL (reader 2, 13/24 [54%]) on axial MPR images of venous phase MR angiography, and only 1/23 [4%] EL (reader 2, 2/24 [8%]) on arterial phase MR angiography.

The overall mean aneurysm size on MDCT, measured perpendicularly to the centerline of the aneurysm, decreased from 56×51 mm (std 11 mm) to 53×48 mm (std 12 mm, $p<0.01$) over a mean follow-up time of 23 months. In 41/43 patients, including 16 patients with endoleaks, comparison with previous CT studies showed stable or decreasing aneurysm dimensions. In two of 43 patients with an

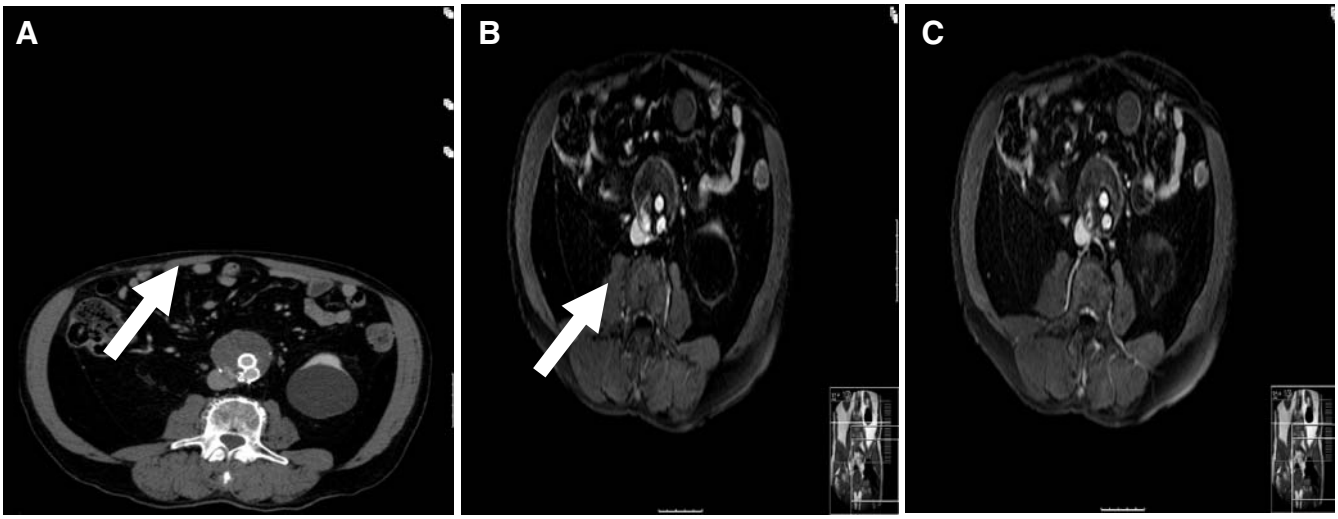

Fig. 3 Type II endoleak in a 74-year-old patient after EVAR. Axial delayed phase CT angiogram (**a**) and contrast-enhanced T1-weighted fast field echo MR image (**b**,**c**) with selective water excitation to suppress the signal from fat (T1 WATS) clearly show a peripheral endoleak (*arrows*). The MR image on the right (**c**) again demonstrates the endoleak located near the ostia of the lumbar arteries, indicating a type II endoleak. The stent graft caused only minor artifacts on both CT (**a**) and MRI (**b**,**c**) studies

indeterminate EL at consensus reading there was a slow increase of 10 mm (9 mm) of maximum diameter size of the aneurysm over a time period of 42 months (38 months). In both cases the endoleaks were also demonstrated on MDCT. Unfortunately, both patients refused digital subtraction angiography to classify and eventually to embolize the endoleak. From the remaining 16 patients with EL detected on consensus reading, 14 showed stable aneurysm size and in 2 patients the dimensions of the aneurysm decreased by 10 mm during follow-up of 5 and 12 months, respectively.

Image quality

Overall Image quality was rated good for MRI (mean score 0.86±0.52) and excellent for CT (mean score 0.33±0.55; $p<0.0001$). Artifacts caused by stent grafts were major for MRI (mean score 1.02±0.41) compared with CT (mean score 0.26±0.58; $p<0.0001$), but minor for coils on MRI (0.33±0.75 for coils) compared with CT (0.95±0.76; $p<0.001$).

The mean patient in-room time for the complete MRI examination was 16.1 min (std 3.3 min, range 13–26 min) for CTA 9.1 min (std 1 min, range 8–10.5 min) ($p<0.0001$)

Discussion

The occurrence of endoleaks represents a major limitation of the endovascular repair of abdominal aortic aneurysms. Identification of endoleaks and their persistence is of great importance to determine prognosis of patients after EVAR.

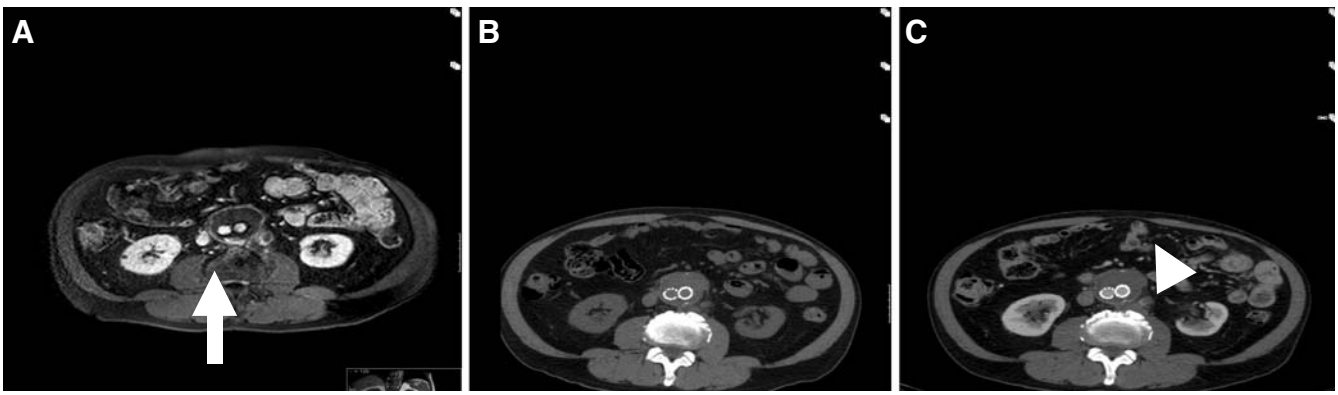

Fig. 4 Peripherally located type II endoleak in a 70-year-old patient after EVAR detected only on axial contrast-enhanced T1-weighted fast field echo MR image with fat suppression (T1 WATS) (**a**, *arrow*), but not visualized on corresponding axial CT angiogram (**c**), neither on arterial (not shown) nor late contrast phase CT (**c**). The linear dense structure visualized on the late phase CTA image (**c**, *arrowhead*) represents a vascular calcification in the posterior aortic wall also shown on the unenhanced CT (**b**)

Table 4 Diagnostic performance of MRI compared with MDCT in the detection of endoleaks in 43 patients after EVAR

	MRI		MDCT	
	Reader 1	Reader 2	Reader 1	Reader 2
TP	20	19	11	12
TN	24	22	25	25
FP	2	5	0	0
FN	0	1	9	8
Sensitivity (%)	100 (90–100) [20/20]	95 (85–100) [19/20]	55 (47–63) [11/20]	60 (52–68) [12/20]
Specificity (%)	92 (84–100) [24/26]	81 (74–88) [22/27]	100 (92–100) [25/25]	100 (92–100) [25/25]
Accuracy (%)	96 (90–100) [44/46]	87 (81–93) [41/47]	80 (75–85) [36/45]	82 (77–88) [37/45]
NPV (%)	100 (92–100) [24/24]	96 (87–100) [22/23]	74 (68–79) [25/34]	76 (70–81) [25/33]

Data are number of endoleaks. Numbers in parentheses () are 95% confidence intervals and number in brackets [ ] were used to calculate percentages
TP true positive, *TN* true negative, *FP* false positive, *FN* false negative, *NPV* negative predictive value.

Only complete exclusion of an aneurysm after endovascular repair can be considered as full success of the procedure, whereas persistence of an EL continues to be a reason for concern since these patients may be at risk for increasing aneurysm size and even rupture [17–20]. Today computed tomography is widely accepted as the principal imaging method for follow-up of patients after EVAR, but this technique is known to have limitations in the detection of EL as highlighted by the phenomenon of endotension and by the difficulty to visualize type II ELs with slow flow [11, 21].

In order to overcome the limitations of CT in the life-long imaging surveillance of patients after EVAR alternative techniques such as color Doppler ultrasonography (CDUS) have been used. This method has been shown to be efficient, when performed by experienced operators, for the detection of small ELs not detected by CT [22, 23]. However, CDUS has the disadvantage that it is strongly operator dependent which may have a negative impact on reproducibility of the results. In addition, poor study quality in obese patients represents another drawback of this method [24].

Recently, the use of gadolinium-enhanced MRI has shown certain potential for follow-up of patient after EVAR resulting in a few studies [10–12, 21, 25–27] with superior detection rates of EL for MRI compared with single- or 4-slice CT.

The current CT protocol consisted in a triphasic data acquisition that has been shown in the literature to be the most reliable for the identification of ELs with most of the EL detected on the late phase images [6]. This finding was in accordance with the results of our study detecting all endoleaks on the delayed phase study but only few on the arterial phase. This observation can be explained by the absence of types I and III ELs which are characterized by high flow and should therefore clearly be evidenced on the arterial phase.

A major finding of our study was the significantly higher number of ELs detected by MRI compared with MDCT for both readers with late phase T1-weighted gadolinium-enhanced MRI being the most efficacious for identification of the endoleak within the aneurysm sac. These results are in accordance with previous studies [10–12, 21, 25–27]. The types of EL matched well between CT and MRI which may be explained by the analogous behavior of EL for both techniques. Compared with CT, MRI identified a major number of type II and indeterminate EL similar to a previous study [11].

Compared with a previous publication by van der Laan and colleagues, we found a slightly lower number of indeterminate EL of 40% at consensus reading versus approximately 60% in the referenced study. There was relatively poor agreement between observers for the classification of EL which reflects the well-known difficulty of categorizing the precise type of EL on both CT and MR imaging [8, 11]. The gold standard for classification of EL remains the digital subtraction angiography (DSA) [3, 7], but this technique is recognized to have a limited sensitivity to identify EL with slow flow [5]. Therefore, MRI and MDCT represent the methods of choice for EL detection, which is reflected by the excellent interobserver agreement, but they are not as specific as DSA for endoleak classification.

The significance of indeterminate EL remains unclear. They may be caused by blood flow through vessels too small to be visualized by present imaging techniques or they may be a consequence of progressive tissue organization with formation of angiogenesis in the excluded aneurysm as supposed by Pitton and coauthors [16]. Taking in account the different MRI protocol used in this animal study including T1-weighted spin echo sequences pre- and post-gadolinium and T2-weighted sequences but no MR angiography, the results of both studies are not directly comparable. The finding in our study that the majority of indeterminate ELs were also identified in the MRA sequence and only a minority exclusively in the late phase post-gadolinium T1 echogradient sequences underlines the hypothesis that a majority of these EL may be

formed by an authentic vascular supply and not by a process of tissue organization [10]. One could only speculate that the vascular supply of these endoleaks could be provided by vasa vasorum of the aortic wall.

The main result of our study was the significantly superior sensitivity of MRI for the detection of endoleaks after EVAR compared with MDCT; however, this finding did not translate into immediate therapeutic consequences for these patients. In fact, none of the ELs undetected on MDCT were associated with an increase in dimensions of the aneurysm size. Therefore, none of our patients underwent DSA for further classification and potential treatment of EL since this examination would not have had any therapeutic consequences considering stability of aneurysm size.

Today, imaging follow-up of patients after EVAR normally includes radiographs of the abdomen and triphasic CT angiography [3, 6]. Considering the necessity of life-long imaging surveillance, these methods are associated with a considerable cumulative radiation exposure and therefore with a potential increase in lifetime cancer mortality risk [28]. Some authors suggest eliminating single phases of the standard triphasic CT protocol to reduce radiation dose [29, 30]; however, there is no generally accepted consensus on this issue. In addition, iodinated contrast material is known to be potentially nephrotoxic. Magnetic resonance imaging does not have the drawback of radiation exposure and is associated with a lower risk of nephrotoxicity. Additionally, it has a higher sensitivity than MDCT for EL detection. MRI should therefore be considered a viable alternative to MDCT for follow-up of patients after EVAR with nitinol stent grafts.

Unlike previously mentioned studies we used gadolinium-BOPTA for MR angiography. This compound differs from standard extracellular contrast agents by its weak and transient interaction with serum albumin leading to an almost twofold increase in T1 relaxivity compared with most conventional gadolinium chelates [31]. In addition, Gd-BOPTA also recently was shown to lead to improved vascular enhancement in more distal vessels in the peripheral circulation as compared with standard extracellular Gd chelates [32] and to delineate significantly more patent vessels than selective DSA in the pedal arteries [33]. Therefore, Gd-BOPTA appears to be advantageous for assessment of endoleaks, especially those small in size and characterized by low flow. Furthermore, we used a slightly higher dose of 0.15 mmol/kg body weight of Gd-BOPTA compared with the standard dose of 0.1 mmol/kg in order to improve endoleak enhancement and detection.

Contrary to the general opinion [4], MRI should not necessarily be considered as a time-consuming imaging method for follow-up after EVAR. The presented MRI protocol was concluded with a mean patient in-room time of only 16 min and 93% (40/43) of MRI studies were completed within 20 min.

A limitation of the present study is the absence of DSA, which is still considered the "gold standard" for classification of endoleaks [7] detected by CT or MRI. However, taking into account the stability of aneurysm size in these patients we did not judge it ethical to perform DSA with the only aim being to better classify the type of EL and without clinical consequences for our patients. Thus, we used consensus reading of both observers evaluating CT and MRI data as the standard of reference, similar to previous studies [10].

Another potential drawback of MRI is that stainless steel stents are ferromagnetic and therefore at risk of migration by the strong magnetic field [3]. In addition, they cause extensive artifacts similarly to elgiloy stents, an alloy of cobalt, chromium, and nickel, which may obscure the stent lumen. Therefore, only patients with nitinol stent grafts should be considered candidates for MRI follow-up.

In conclusion, the described MRI protocol using a high-relaxivity contrast agent provided a significantly higher sensitivity for the detection of endoleaks compared with 16-slice MDCT in patients after endovascular repair of abdominal aortic aneurysms with a nitinol stent graft. Therefore, the rates of endoleaks after EVAR depend substantially on the imaging method used. In addition, considering the lack of radiation, the lower nephrotoxicity of the MR contrast agent at the clinically approved dose, and the relatively short examination time, magnetic resonance imaging may become the preferred imaging investigation for patient follow-up after endovascular repair of abdominal aortic aneurysms.

Acknowledgments Rolf Wyttenbach, MD, is supported by a grant from the Swiss Heart Foundation. We thank Paolo Santini, RT, and the team of MRI technicians for their collaboration and support.

References

1. Parodi JC, Palmaz JC, Barone HD (1991) Transfemoral intraluminal graft implantation for abdominal aortic aneurysm. Ann Vasc Surg 5:491–499
2. Zarins CK, Wolf YG, Lee WA et al (2000) Will endovascular repair replace open surgery for abdominal aortic aneurysm repair? Ann Surg 232:501–507
3. Stavropoulos SW, Charagundla SR (2007) Imaging techniques for detection and management of endoleaks after endovascular aortic aneurysm repair. Radiology 243:641–655
4. Eliason JL, Upchurch GR Jr (2008) Endovascular abdominal aortic aneurysm repair. Circulation 117:1738–1744
5. Görich J, Rilinger N, Sokiranski R et al (1999) Leakages after endovascular repair of aortic aneurysm: classification based on findings at CT, angiography and radiography. Radiology 213:767–772

6. Rozenblit AM, Patlas M, Rosenbaum AT et al (2003) Detection of endoleaks after endovascular repair of abdominal aortic aneurysm: value of unenhanced and delayed helical CT acquisition. Radiology 227:426–433
7. Stavropoulos SW, Clark TWI, Carpenter JP et al (2005) Use of CT angiography to classify endoleaks after endovascular repair of abdominal aortic aneurysm. J Vasc Interv Radiol 16:663–667
8. Cherniak V, Rozenblit AM, Patlas M et al (2006) Type II endoleak after endoaortic graft implantation: diagnosis with helical CT angiography. Radiology 240:885–893
9. Wicky S, Fan CM, Geller SC et al (2003) MR angiography of endoleak with inconclusive concomitant CT angiography. Am J Roentgenol 181:736–738
10. Pitton MB, Schweitzer H, Herber S et al (2005) MRI versus helical CT for endoleaks detection after endovascular aneurysm repair. Am J Roentgenol 185:1275–1281
11. Van der Laan MJ, Bartels LW, Viergever MA et al (2006) Computed tomography versus magnetic resonance imaging of endoleaks after EVAR. Eur J Vasc Endovasc Surg 32:361–365
12. Haulon S, Lions C, Mc Fadden EP et al (2001) Prospective evaluation of magnetic resonance imaging after endovascular treatment of infrarenal aortic aneurysm. Eur J Vasc Endovasc Surg 22:62–69
13. Cavagna FM, Maggioni F, Castelli PM et al (1997) Gadolinium chelates with weak binding to serum proteins; a new class of high-efficiency, general purpose contrast agents for magnetic resonance imaging. Invest Radiol 32 (12):780–796
14. Bonvini RF, Alerci M, Antonucci F et al (2003) Preoperative embolization of collateral side branches: a valid means to reduce type II endoleak after endovascular AAA repair. J Endovasc Ther 10:227–232
15. Willinek WA, Gieseke J, Conrad R et al (2002) Randomly segmented central k-space ordering in high-spatial-resolution contrast-enhanced MR angiography of the supraaortic arteries: initial experience. Radiology 225 (2):583–588
16. Pitton MB, Schmenger PR, Neufang A et al (2002) Endovascular aneurysm repair: magnetic resonance monitoring of histoloigical organization process in the excluded aneurysm. Circulation 105:1995–1999
17. Zarins CK, White RA, Fogaty TJ (2000) Aneurysm rupture after endovascular repair using the AneuRx stent graft. J Vasc Surg 31:960–970
18. Politz JK, Newman VS, Stewart MT (2000) Late abdominal aortic aneurysm rupture after AneuRX repair: a report of three cases. J Vasc Surg 31:599–606
19. White RA, Donayre C, Walot I et al (2000) Abdominal aortic aneurysm rupture following endoluminal graft deployment: report of a predictable event. J Endovasc Ther 7:257–262
20. Hinchliffe RJ, Singh-Ranger R, Davidson IR et al (2001) Rupture of an aortic aneurysm secondary to type II endoleak. Eur J Vasc Endovas Surg 22:563–565
21. Cejna M, Loewe C, Schoder M et al (2002) MR angiography vs CT angiography in the follow-up of nitinol stent grafts in endoluminal treated aortic aneurysm. Eur Radiol 12:2443–2450
22. Sato DT, Goff CD, Gregory RT et al (1998) Endoleak after aortic stent repair: diagnosis by color duplex ultrasound scan versus computed tomography scan. J Vasc Surg 28:657–663
23. Napoli V, Bargellini I, Sardella SG et al (2004) Abdominal aortic aneurysm: contrast enhanced US for endoleak after endoluminal repair. Radiology 233:217–225
24. Pitton MB (2005) Diagnosis and management of endoleaks after endovascular aneurysm repair: role of MRI. Abdom Imaging 31:339–346
25. Engellau L, Larsson EM, Albrachtsson U et al (1998) Magnetic resonance imaging and MR angiography of endoluminal treated abdominal aortic aneurysm. Eur J Vasc Endovasc Surg 15:212–219
26. Insko EK, Kulzer LM, Fairman RM et al (2003) MR imaging for detection of endoleaks in recipients of abdominal aortic stent-grafts with low magnetic susceptibility. Acad Radiol 10:509–513
27. Ayuso JR, de Caralt TM, Pages M et al (2004) MRA is useful as follow-up technique after endovascular repair of aortic aneurysm with nitinol endoprosthesis. J Magn Reson Imaging 20:803–810
28. Brenner DJ, Elliston CD (2004) Estimated radiation risks potentially associated with full-body CT screening. Radiology 232:735–738
29. Iezzi R, Cotroneo AR, Filippone A et al (2006) Multidetector CT in abdominal aortic aneurysm treated with endovascular repair: are unenhanced and delayed phase enhanced images effective for endoleak detection. Radiology 241 (3):915–921
30. Macari M, Chandarana H, Schmidt B et al (2006) Abdominal aortic aneurysm: can the arterial phase at CT evaluation after endovascular repair be eliminated to reduce radiation dose. Radiology 241 (3):908–914
31. De Haen C, Cabrini M, Akhnana L et al (1999) Gd-BOPTA 0.5M solution for injection (MultiHance®): pharmaceutical formulation and physicochemical properties of a new magnetic resonance imaging contrast medium. J Comput Assist Tomogr 23(Suppl 1):S161–S168
32. Wyttenbach R, Gianella S, Alerci M et al (2003) Prospective blinded evaluation of Gd-DOTA- versus Gd-BOPTA-enhanced peripheral MR angiography, as compared with digital subtraction angiography. Radiology 227:261–269
33. Kreitner KF, Kunz RP, Herber S et al (2008) MR angiography of the pedal arteries with gadobenate dimeglumine, a contrast agent with increased relaxivity, and comparison with selective intraarterial DSA. J Magn Reson Imaging 27(1):78–85